

# Synthesis of Deep-Red-Emitting CdSe Quantum Dots and General Non-Inverse-Square Behavior of Quantum Confinement in CdSe Quantum Dots

Qiangbin Wang and Dong-Kyun Seo\*

Department of Chemistry and Biochemistry, Arizona State University, Tempe, Arizona 85287-1604

Received May 5, 2006. Revised Manuscript Received September 6, 2006

High-quality red-emitting CdSe quantum dots were synthesized by a microwave-assisted heating method in which the particle size was controlled mainly by changing reaction temperatures from 190 to 270 °C. The prepared samples were characterized by XRD, UV–Vis, photoluminescence, and TEM methods. The particle sizes range from 6.0 to 13.4 nm beyond the strong quantum confinement regime. The smallest quantum dots exhibit a zinc-blende structure while larger particles show a wurtzite structure. All the particles are isotropic in shape and exhibit well-defined photoluminescence despite their large sizes. By examining the optical properties of the red-emitting CdSe quantum dots, a definite quantification of size dependence of optical band gap with a clear empirical  $1/d^{1.25}$  scaling in a broad size range including smaller particles was established.

## Introduction

The colloidal CdSe quantum dots (QDs) are one of the most extensively investigated nanostructures due to their size-dependent optical band gaps<sup>1–9</sup> tunable across the visible spectrum as well as the established synthetic methodologies.<sup>10–15</sup> From the previous studies, observed size dependence of optical properties of CdSe QDs has been well-documented for the QDs that are far within the strong quantum confinement regime,  $d \ll 2a_B = \sim 10$  nm, where  $d$  and  $a_B$  are the diameter of the QDs and the average exciton Bohr radius of the bulk CdSe, respectively. However, systematic studies on the larger CdSe QDs have been relatively scarce probably because of their limited availability beyond the strong quantum confinement regime. Such large CdSe particles tend to exhibit anisotropic rod shapes frequently with rather broad distributions in size and/or aspect ratio and show inappreciable photoluminescence (PL) efficiency.<sup>16–19</sup> Such problems can hamper the studies of

quantum confinement of large CdSe QDs near the medium or weak confinement regime and furthermore the establishment of a general quantum confinement scaling behavior from small to large QDs. In this work, we report optical behavior of spherical red-emitting CdSe QDs up to the true red emission wavelengths ( $\sim 700$  nm) and establish the size dependence of the band gaps in the large CdSe QDs. As a result, our findings extend the quantification of the quantum confinement to the largest CdSe QDs up to 13.4 nm in diameter and allow a new description of the behavior of  $\Delta E_g$  (the increase in the optical band gap above the bulk value) vs  $d$  for CdSe QDs in a *broad* size range.

To a first approximation, the size dependence of QDs is in general described by a simple particle-in-a-box model that predicts  $\Delta E_g \propto 1/d^2$  (inverse-square behavior) based on an effective-mass approximation.<sup>1</sup> Significant deviations found in the experimental data have been attributed to the breakdown of the approximation or simplistic choice of the QD boundary condition for small QDs and to the increasing importance of the Coulombic interactions for large QDs.<sup>4</sup> More recent works have pointed out that the particle-in-a-box models do not predict the absolute slope values and nonzero intercepts in  $\Delta E_g$  vs  $1/d^2$  plots obtained for InP QDs and quantum wires (QWs).<sup>20</sup> From empirical fitting,  $\Delta E_g$  values were found to be proportional to  $1/d^n$  ( $n = 1.35$  and  $1.45$  for InP QDs and wires) instead, which is consistent with the semiempirical pseudopotential calculation results.<sup>21,22</sup> To the contrary, other calculation results based on the charge patching method did not differentiate QDs from QWs in the

- (1) Brus, L. E. *J. Chem. Phys.* **1984**, *80*, 4403.
- (2) Brus, L. *J. Phys. Chem.* **1986**, *90*, 2555.
- (3) Efros, Al. L. *Phys. Rev. B* **1992**, *46*, 7448.
- (4) Norris, D. J.; Bawendi, M. G. *Phys. Rev. B* **1996**, *53*, 16338.
- (5) Efros, Al. L.; Rosen, M.; Kuno, M.; Nirmal, M.; Norris, D. J.; Bawendi, M. G. *Phys. Rev. B* **1996**, *54*, 4843.
- (6) Leung, K.; Pokrant, S.; Whaley, K. B. *Phys. Rev. B* **1998**, *57*, 12291.
- (7) Efros, Al. L.; Rosen, M. *Annu. Rev. Mater. Sci.* **2000**, *30*, 475.
- (8) Wang, L.-W.; Zunger, A. *Phys. Rev. B* **1996**, *53*, 9579.
- (9) Wang, L.-W.; Li, J. *Phys. Rev. B* **2004**, *69*, 153302.
- (10) Murray, C. B.; Norris, D. J.; Bawendi, M. G. *J. Am. Chem. Soc.* **1993**, *115*, 8706.
- (11) Peng, X.; Wickham, J.; Alivisatos, A. P. *J. Am. Chem. Soc.* **1998**, *120*, 5343.
- (12) Aldana, J.; Wang, Y. A.; Peng, X. *J. Am. Chem. Soc.* **2001**, *123*, 8844.
- (13) Talapin, D. V.; Rogach, A. L.; Kornowski, A.; Hasse, M.; Weller, H. *Nano Lett.* **2001**, *1*, 207.
- (14) Qu, L.; Peng, Z. A.; Peng, X. *Nano Lett.* **2001**, *1*, 333.
- (15) Qu, L.; Peng, X. *J. Am. Chem. Soc.* **2002**, *124*, 2049.
- (16) Peng, X.; Manna, L.; Yang, W.; Wickham, J.; Scher, E.; Kadavanich, A.; Alivisatos, A. P. *Nature* **2000**, *404*, 59.
- (17) Hu, J.; Li, L.-S.; Yang, W.; Manna, L.; Wang, L.-W.; Alivisatos, A. P. *Science* **2001**, *292*, 2060.

- (18) Katz, D.; Wizansky, T.; Millo, O.; Rothenberg, E.; Mokari, T.; Banin, U. *Phys. Rev. Lett.* **2002**, *89*, 086801.
- (19) Shieh, F.; Saunders, A. E.; Korgel, B. A. *J. Phys. Chem. B* **2005**, *109*, 8538.
- (20) Yu, H.; Li, J.; Loomis, R. A.; Wang, L.-W.; Buhro, W. E. *Nat. Mater.* **2003**, *2*, 517.
- (21) Fu, H.; Zunger, A. *Phys. Rev. B* **1997**, *56*, 1496.
- (22) Li, J.; Wang, L.-W. *Chem. Mater.* **2004**, *16*, 4012.

$1/d^n$  scaling.<sup>23</sup> For both dots and wires,  $n$  was estimated to be 1.1 in the InP system and 1.2 in the CdSe. Indeed, such nonlinear behaviors have been observed experimentally for CdSe quantum wells<sup>24</sup> and quantum wires<sup>20</sup> that are relatively large in thickness and diameter, respectively. That is, the QWs of relatively large diameters were found to scale linearly with  $1/d^{1.36}$  in experimental data, and this was consistent with semiempirical pseudopotential calculation results.<sup>20</sup> For the CdSe QDs, furthermore, previous semiempirical pseudopotential calculations have predicted a  $1/d^{1.35}$  behavior based on the results for small QDs with  $d < 4$  nm.<sup>8</sup> From the experimental side, empirical scaling  $1/d^n$  for CdSe QDs has not been reported yet in the literature, although for the particles smaller than 6 nm an exponential relationship has been made between PL  $\lambda_{\max}$  and  $d$ .<sup>15</sup> Extending the large size limit of available CdSe QDs can thus be important for experimental quantification of the  $1/d^n$  scaling. Indeed, large CdSe QDs up to 11.5 nm was reported in an early seminal work, and yet their photoluminescence and shapes were not described.<sup>10</sup> To our knowledge, there have been no further systematic studies on large isotropic CdSe QDs until now.

### Experimental Section

Five different samples of oleylamine-capped CdSe QDs were obtained by employing the low-temperature synthetic method previously reported by us.<sup>25,26</sup> Handling of the chemicals and solutions was carried out in a nitrogen-filled glovebox except during the postsynthesis processes. In a typical synthetic process, 0.2 mmol of  $B_2Se_3$  and 0.6 mmol of  $CdCl_2$  were loaded into 3 mL of oleylamine in separate sealed vials and dissolved by heating at 110 °C for 20 min. After the solutions were cooled down, they were mixed together and divided into three 15-mL crimp-top microwave-reaction vials. The vials were tightly sealed using an aluminum crimp cap with Teflon-lined rubber septum before being taken out from the glovebox. Each mixture solution was heated at 190, 200, 210, 230, or 270 °C for 60 s at 300 W in a CEM microwave reactor, and the different reaction temperatures provided products with different emission wavelengths but all in red. The emission peak of as-prepared CdSe QDs has a full-width at half-maximum (fwhm) from 45 to 52 nm. It is pointed out that in our experiments the size control was achieved by changes in reaction temperatures rather than the reaction time in contrast to the conventional high-temperature TOPO/TOPSe method.

The CdSe QDs are freely soluble in toluene and are precipitated in alcohol solution. Size-selective precipitation allowed narrower size distributions based on the fwhm (30–40 nm) of the emission peak. Further characterization was carried out with the final products (Table 1). The size and shape of the CdSe QD products were examined with an FEI Tecnai F20 transmission electron microscope by inspecting at least six different regions in the same sample holder for each product. The particle diameters were measured individually for 180–250 combined numbers of particles from several micrographs per specimen, and their average values and standard deviations were obtained through a conventional statistical analysis of population. The optical spectra were measured with Shimadzu UV-2100U spectrophotometer and Jobin Yvon Fluoromax-3 Spec-

**Table 1. Size and Optical Characteristics of the Red-Emitting CdSe QDs**

size <sup>a</sup> (nm)	size dispersity <sup>a</sup> (%)	$\lambda_{\text{abs}}^b$ (nm)	PL $\lambda_{\text{max}}$ (nm)	fwhm (nm)	QY (%)
6.0	5	634	648	31	8.8
7.2	7	648	659	34	1.9
8.8	10	661	672	39	1.1
10.5	7	672	683	35	1.4
13.4	9	681	698	39	0.75

<sup>a</sup> Estimated from TEM images. <sup>b</sup> Lowest energy excitonic peaks were extracted by nonlinear least-squares fitting and background subtraction.

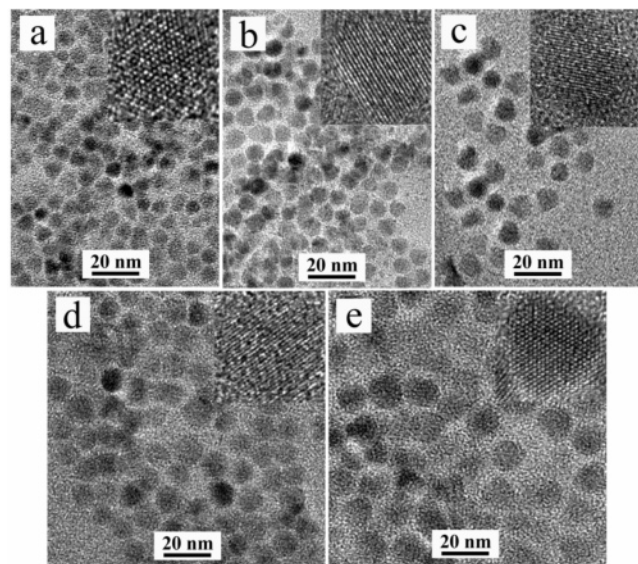


**Figure 1.** Representative transmission electron micrographs of the oleylamine-capped red-emitting CdSe QDs. Higher magnification images of individual dots are shown in the insets. The samples a, b, c, d, and e were prepared at 190, 200, 210, 230, and 270 °C, respectively.

trofluorometer, respectively. The maximum position ( $\lambda_{\text{abs}}$ ) of the lowest energy excitonic peaks was extracted from the absorption spectra by nonlinear least-squares fitting and background subtraction as suggested previously.<sup>20,23</sup> To be specific, each spectrum was fit in the region of 550–750 nm with multiple Gaussian functions using Origin 7.0 nonlinear least-squares-fitting software (www.OriginLab.com). The number of Gaussian functions used was determined by adding Gaussians until the residual was structureless and also until the fitting parameters were changed negligibly upon addition of more Gaussian functions. (The background was a partial Gaussian.) The longest wavelength peak in the spectrum was the lowest energy Gaussian component of the fit. The fitting procedure yielded the center wavelength of this excitonic peak and the error in the center wavelength. A greater error than that suggested by the peak fitting was actually used; the assumed error was  $\pm 1$  nm ( $\sim 0.005$  eV).

### Results and Discussion

Figure 1 shows TEM images of the CdSe nanocrystals obtained in our experiments. Overall, the particles have isotropic shapes with relatively homogeneous size distributions (5–10%). The spherical shapes found in our samples are pertinent to unambiguous investigation of size effect. The average size and size dispersity are listed in Table 1. The insets in Figure 1 show high-resolution TEM images of well-developed lattice fringes in the CdSe nanoparticles, indicating a good crystallinity of all the samples. The X-ray diffraction

(23) Yu, H.; Li, J.; Loomis, R. A.; Gibbons, P. C.; Wang, L.-W.; Buhro, W. E. *J. Am. Chem. Soc.* **2003**, *125*, 16168.

(24) Mikhailov, G. V.; Panfilov, A. G.; Razbirin, B. S. *J. Cryst. Growth* **1990**, *101*, 739.

(25) Iancu, N.; Sharma, R.; Seo, D.-K. *Chem. Commun.* **2004**, *20*, 2298.

(26) Wang, Q.; Iancu, N.; Seo, D.-K. *Chem. Mater.* **2005**, *17*, 4762.

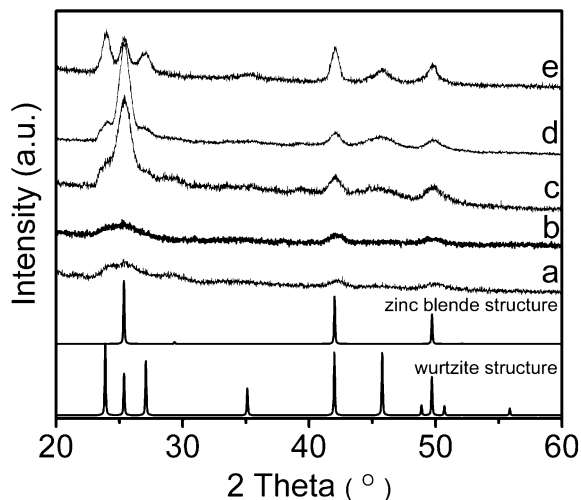


**Figure 2.** XRD patterns of the CdSe QD samples. a, b, c, d, and e were prepared at 190, 200, 210, 230, and 270 °C, respectively. The simulated patterns of bulk CdSe in zinc blende<sup>29</sup> and wurtzite structures<sup>30</sup> are shown at the bottom as reference.

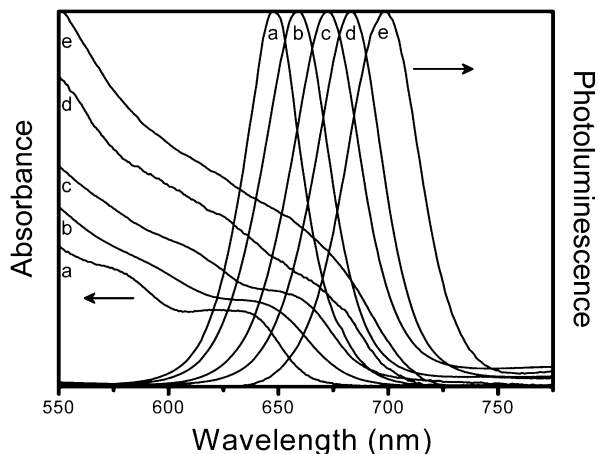


**Figure 3.** Absorption and PL spectra of the CdSe QDs in toluene. The samples a, b, c, d, and e were prepared at 190, 200, 210, 230, and 270 °C, respectively. For the PL studies, the solution samples were excited at 365 nm.

patterns (XRD) also indicate their crystallinity in bulk (Figure 2). The CdSe nanocrystals exhibit zinc-blende-type crystal structure under the low-temperature conditions, which is consistent with our previous results.<sup>25,26</sup> The structure type of the QDs gradually changes from zinc blende to wurtzite as reaction temperature increases. However, the assignment of the zinc-blende-type structure may not be clear because stacking faults in the wurtzite-type structure can cause “zinc-blende-like” X-ray diffraction patterns at least for very small CdSe particles with a diameter of  $\sim 3\text{--}4$  nm.<sup>27</sup> It has been known that there is no noticeable difference in optical properties between the two types of CdSe QDs.<sup>15,27</sup>

Figure 3 shows the absorption and PL spectra under a 365 nm excitation wavelength of the five different CdSe QD samples. The PL quantum yields (QYs) of the QD products were 8.8, 1.9, 1.1, 1.4, and 0.75%,<sup>28</sup> with  $\lambda_{\text{max}} = 648, 659, 672, 683,$  and  $698$  nm, respectively. The corresponding PL

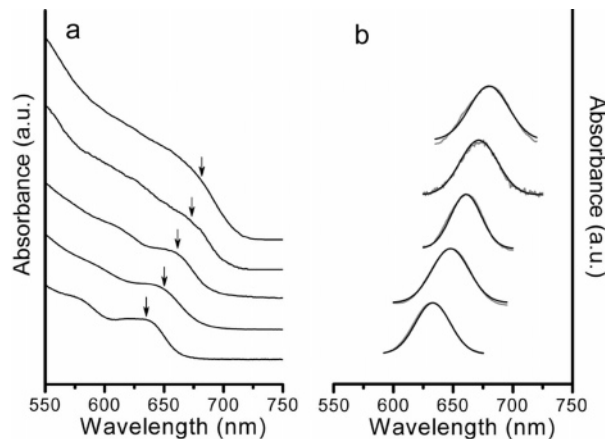


**Figure 4.** (a) Absorption spectra of the CdSe QDs. The vertical arrows mark the peak maximum of the lowest energy excitonic absorptions that were found from nonlinear least-squares fitting. (b) Lowest energy excitonic peaks (gray curves) extracted by nonlinear least-squares fitting and background subtraction, and the Gaussian fits to those peaks (black curves).<sup>20,23</sup>

fwhm values of the samples were 31, 34, 39, 35, and 39 nm. The PL QYs showed a decreasing tendency with the increase in the QD sizes, which is consistent with others' results.<sup>13,14</sup> Namely, the overlap between electron and hole wavefunctions in an electron–hole pair becomes smaller on increasing particle size, leading to a reduced radiative rate and, as a result, decreased QY.<sup>29</sup> Nevertheless, the PL emission of the samples was clearly visible to the naked eyes upon the excitation by a conventional UV lamp. In Figure 4a, the locations of the lowest excitonic peak maximum are indicated by arrows on the absorption spectra as obtained from the fitting procedure described in the previous section. Those extracted excitonic peaks (gray) were compared in Figure 4b with the Gaussian fits (black). Red shifts of optical band gaps and PL maxima are obvious in Figures 3 and 4 as the particle size increases. Table 1 summarizes the optical properties of the samples along with the size characteristics.

In Figure 5,  $\Delta E_g$  values<sup>30</sup> for the CdSe QDs from our synthesis were plotted vs  $1/d^2$  in addition to two data sets (open diamonds<sup>10,23</sup> and solid circles<sup>11</sup>) from previous works. For the sake of consistency for the large-size CdSe QDs shown in open diamonds, we employed the literature data<sup>23</sup> that were from the same nonlinear least-squares fitting procedure employed in our work. The  $\Delta E_g$  values in solid squares (present work) correlate to the previous results (open diamonds) in the large-size region above 5 nm. In the inset of Figure 5, however, a deviation of the  $\Delta E_g$  values in solid squares is clearly noticeable from the inverse-square behavior, as the  $\Delta E_g$  values are not aligned well to the dashed line that is reproduced from the particle-in-a-box model.<sup>1</sup> More significantly, it is recognized that, in the *entire* size range,  $\Delta E_g$  is not linearly dependent on  $1/d^2$  for all three independent data sets, diverging from the particle-in-a-box model. This digression is more severe for smaller particles, which was indeed indicated in the original work where the

(27) Bawendi, M. G.; Kortan, A. R.; Steigerwald, M. L.; Brus, L. E. *J. Chem. Phys.* **1989**, *91*, 7282.

(28) For quantum yield calculations, see, for example: Crosby, G. A.; Demas, J. N. *J. Phys. Chem.* **1971**, *75*, 991.

(29) Kan, S.; Mokari, T.; Rothenberg, E.; Banin, U. *Nat. Mater.* **2003**, *2*, 155.

(30)  $\Delta E_g = E_g^{\text{QD}} - E_g^{\text{bulk}}$ . For wurtzite CdSe,  $E_g^{\text{bulk}} = 1.74$  eV at 300 K. See, Madelung, O. *Semiconductors: Data Handbook*, 3rd ed.; Springer-Verlag: Berlin, Germany, 2004; p 228.

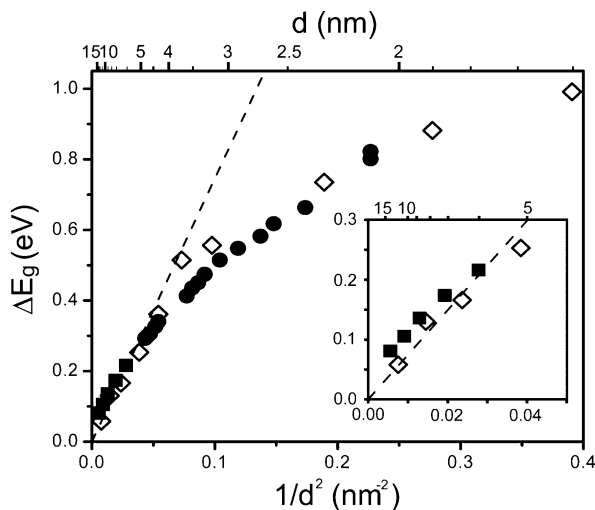


**Figure 5.** Experimental CdSe QD data plotted as  $\Delta E_g$  vs  $1/d^2$ . Square, diamond, and circle symbols indicate the  $\Delta E_g$  from our experiments, refs 10 and 23, and ref 11, respectively. The dashed line was reproduced from a particle-in-a-box model.<sup>1</sup> The large-size region ( $d > 5$  nm) is magnified in the inset.

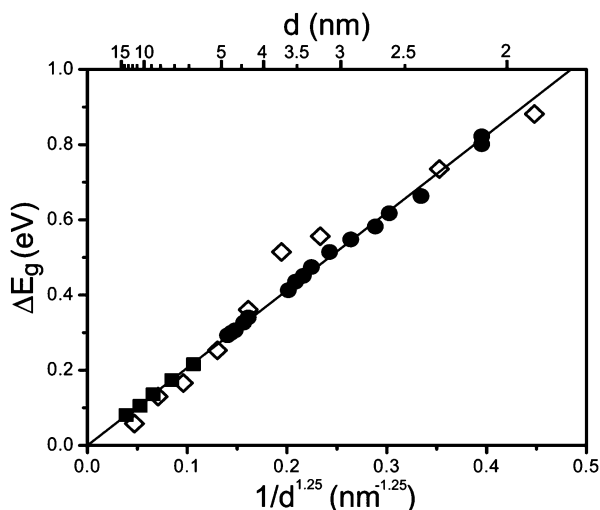


**Figure 6.** Experimental CdSe QD data plotted as  $\Delta E_g$  vs  $1/d^{1.25}$ . For the convention of the symbols, see Figure 5. The solid line is the least-squares fits to the experimental values of the  $\Delta E_g$  values in squares and circles.

digression was indicated to be caused by nonparabolicity of bands at higher wave vectors and the finite potential barrier at the surface of the particles. Upon the deviation observed even for the larger size QDs, however, our attempt was to obtain an empirical relationship between  $\Delta E_g$  and  $d$  that can be applicable for the entire size range of the particles reportedly previously and in our current work.

Empirical fitting over the entire size range indicated that the  $\Delta E_g$  values are proportional to  $1/d^{1.28 \pm 0.04}$  with a slope  $A = 2.1 \pm 0.1$ . However, the most precise parameters, i.e.,  $n = 1.251 \pm 0.008$  and  $A = 2.06 \pm 0.02$ , were obtained when the same fitting procedure was employed only for the experimental values from the present work (solid squares) and from the values in solid circles.<sup>11</sup> Consequently, the  $\Delta E_g$  values were plotted vs  $1/d^{1.25}$  in Figure 6, in which the

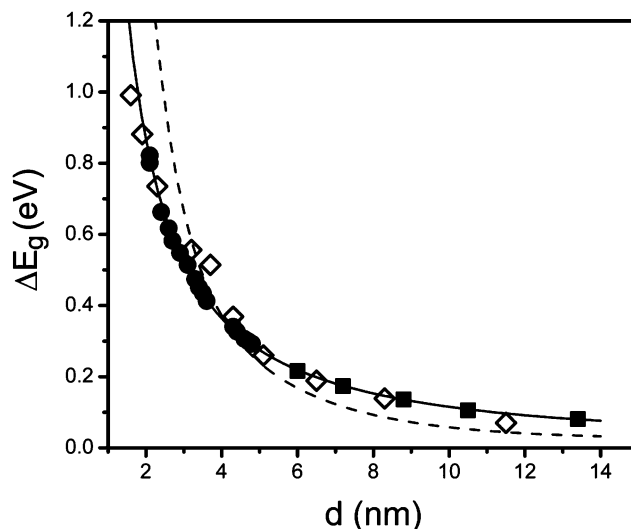


**Figure 7.** Experimental CdSe QD data plotted as  $\Delta E_g$  vs  $d$ . For the convention of the symbols, see Figure 5. The dashed line was reproduced from a particle-in-a-box model. The solid line is the least-squares fits to the experimental values of the  $\Delta E_g$  values in squares and circles.

previous  $\Delta E_g$  values in open diamonds were also shown for comparison. The excellent linear relationship in the  $\Delta E_g$  vs  $1/d^{1.25}$  plot indicates that the size dependence of the optical band gaps of the CdSe QDs is different from that of the corresponding QWs ( $n = 1.25$  vs  $1.36$ ). Figure 7 also shows clearly the agreement between the fitted relationship (solid line) and experimental data (black circles/squares and open diamonds) and the deviation of the particle-in-a-box model (dashed line) in both small- and large-size regions. While no further speculations are made, it is curious to note that the difference in  $n$  between the CdSe QWs and QDs ( $1.36 - 1.25 = 0.11$ ) is practically identical to the difference found in the InP system ( $1.45 - 1.35 = 0.10$ ).

### Concluding Remarks

We have successfully prepared and characterized high-quality CdSe quantum dots of large sizes from 6.0 to 13.4 nm in diameter. Our work extended the experimental quantification of the size dependence of the optical band gaps and allowed us to establish that the  $\Delta E_g$  values scale linearly with  $1/d^{1.25}$  over a broad size range. We suspect that our findings may provide a valuable signpost for the studies of quantum confinements in the CdSe system as well as in others.

**Acknowledgment.** D.-K.S. is grateful for financial support from the National Science Foundation through his CAREER Award (DMR - Contract No. 0239837) and for his Camille Dreyfus Teacher-Scholar Award from the Camille and Henry Dreyfus Foundation. The authors thank Dr. Renu Sharma for her TEM imaging and Mr. Fudong Wang for his valuable help in nonlinear least-squares fitting of the absorption spectra.

CM061051J